



Influence of the support composition on the hydrogenation of methyl acetate over Cu/MgO-SiO₂ catalysts

Hongyun Qin, Cuili Guo*, Chengwei Sun, Jinli Zhang

School of Chemical Engineering and Technology, Tianjin University, Tianjin 300072, PR China



ARTICLE INFO

Article history:

Received 25 November 2014

Received in revised form 9 July 2015

Accepted 10 July 2015

Available online 17 August 2015

Keywords:

Ethanol

Methyl acetate

Hydrogenation

Magnesium oxide

ABSTRACT

A series of Cu/MgO-SiO₂ catalysts with different support compositions of MgO and SiO₂ were prepared using the ammonia-evaporation method and evaluated for methyl acetate hydrogenation reaction to synthesize ethanol. Physicochemical properties of these catalysts were investigated by N₂ physisorption, N₂O chemisorptions, X-ray diffraction, H₂-temperature programmed reduction, CO₂-temperature programmed desorption and X-ray photoelectron spectroscopy. It was found that the MgO content significantly influenced the chemical properties, then affected catalytic activities of Cu/xMgO-SiO₂ catalysts. The optimal catalytic performance was obtained over Cu/9MgO-SiO₂ catalyst with MgO/SiO₂ mass ratio of 9 with the methyl acetate conversion of 80.3% and ethanol selectivity of 99.0%. The high catalytic performance of Cu/9MgO-SiO₂ catalyst was attributed to the fine copper dispersion and large amount of weakly basic sites and Cu⁺ species.

© 2015 Elsevier B.V. All rights reserved.

1. Introduction

Ethanol, one of the most widely used chemical raw materials, is applied to diverse industries, such as chemical, pharmaceutical, coating food industries, etc. In particular, ethanol as an alternative energy source will hold great promise [1–4]. Ethanol is commercially produced via two routes, fermentation of sugars and hydration of ethylene. However, fermentation of sugars and hydration of ethylene will face great challenges owing to the lack of food supplies and the worldwide oil crisis. Hence, it is necessary to explore new methods that can supplement these resources to meet the increasing demands of ethanol in the future. At present, one of ethanol productive processes arising significant interest is the hydrogenation of methyl acetate (MeOAc), since the process can solve acetic acid (AcOH) overcapacity and avoid the requirement for expensive equipment comparing with AcOH hydrogenation.

For ester hydrogenation, chromium oxide modified Cu-based catalysts exhibit excellent catalytic activities and are widely used. However, the environmental hazard caused by the loss of chromium limits its practical applications. Therefore, it is essential to explore efficient chromium-free catalysts for ester hydrogenation reactions. Recently, Zhu et al. [5,6] reported Cu-Zn/SiO₂ and Cu-Zn/Al₂O₃ catalysts for the hydrogenation of ethyl acetate, and the ethanol yields were 76.5% and 63.2%, respectively. Wang et al.

[7] studied the activities of Cu_x-Zn_y-O catalysts for hydrogenation of methyl acetate and found that the catalytic activities were dependent on the Cu/Zn ratio. The methyl acetate conversion of 72.6% could be obtained on Cu_{0.4}-Zn_{0.6}-O catalyst, better than other catalysts with other Cu/Zn ratio. Some of new and highly effective catalysts were also found during the hydrogenation of dimethyl oxalate [8–11]. These studies show that Cu-based catalysts are active in the hydrogenation of acetate esters to ethanol. However, the catalytic activity and stability still need to improve.

Cu-MgO catalysts are widely applied in many catalytic reaction processes such as low-temperature methanol synthesis from syngas [12,13], hydrogenation of furfural to furfuryl alcohol [14–15] and selective hydrogenolysis of glycerol to 1,2-propanediol [16]. These reports showed that Cu/MgO catalysts could exhibit excellent catalytic performance for hydrogenation reactions. Tu and Chen [17] reported the catalytic activities of different alkaline-earth oxide modified Cu/SiO₂ catalyst for the dehydrogenation of ethanol, the magnesium oxide modified Cu/SiO₂ catalyst exhibited excellent activity and stability, better than other alkaline-earth oxide modified catalysts. Till now, a detailed study on Cu/MgO-SiO₂ catalysts for methyl acetate hydrogenation to ethanol is yet to be published.

In this paper, the MgO-modified Cu/SiO₂ catalysts with different magnesium oxide content were prepared using an ammonia-evaporation method, and their catalytic performances for hydrogenation of methyl acetate were evaluated in fixed-bed reactor. In addition, several characterization techniques including N₂ physisorption, N₂O titration, X-ray diffraction (XRD), H₂-temperature programmed reduction (TPR), CO₂-temperature

* Corresponding author. Fax: +86 22 2270 4495.

E-mail address: gcl@tju.edu.cn (C. Guo).

programmed desorption (CO_2 -TPD), and X-ray photoelectron spectroscopy (XPS) were performed to investigate the influence of magnesium oxide content on the physical properties and chemical properties of the catalysts.

2. Material and methods

2.1. Catalyst preparation

A series of $\text{Cu}/x\text{MgO-SiO}_2$ catalysts with the copper loading of 30 wt% were manufactured via the ammonia-evaporation method. The ammonia aqueous solution, $\text{Mg}(\text{NO}_3)_2 \cdot 6\text{H}_2\text{O}$, $\text{Cu}(\text{NO}_3)_2 \cdot 3\text{H}_2\text{O}$, silica sol were purchased from Tianjin Guangfu Fine Chemical Institute, China. The preparation procedures were as follows. Dissolving 5.66 g of $\text{Cu}(\text{NO}_3)_2 \cdot 3\text{H}_2\text{O}$ and a certain amount of $\text{Mg}(\text{NO}_3)_2 \cdot 6\text{H}_2\text{O}$ in deionized water under the continuous stirring at room temperature. Then the silica sol with amount of 30 wt% was added and mixed for 10 min. Afterwards, a certain amount of 30 wt% ammonia aqueous solution was added and mixed for 3 h. The pH of suspension was kept about 11. Then the suspension was placed in the 368 K water bath to remove the excess ammonia. This progress was terminated at a pH of around 6. The precipitate was aged for 3 h under the room temperature, then calcined at 723 K for 3 h after drying at 393 K for 12 h. The prepared catalyst was named $\text{Cu}/x\text{MgO-SiO}_2$ ($x = 1, 3, 9$ and 20), where x stands for MgO/SiO_2 mass ratio. For comparison, MgO and SiO_2 supported catalysts were also prepared with the same method.

2.2. Catalytic activity tests

The catalytic performances were assessed using a fixed-bed tubular reactor (the tube's inner diameter of 10 mm). Typically, 1.5 g catalyst (60–80 meshes) precursor was mixed with a certain amount of quartz sand (40–60 meshes) and placed in the tubular reactor. The two thermocouples were inserted into the gasification chamber and reactor respectively, for better controlling the temperature. The catalysts were activated at the temperature of 623 K for 4 h by a heating rate of 5 K min^{-1} in a hydrogen atmosphere (150 ml min^{-1}). When cooling to the reaction temperature, methyl acetate (purchased from Tianjin Guangfu Fine Chemical Institute of China) was injected into the gasification chamber of 533 K using a constant flow pump. Then the hydrogen and the methyl acetate were mixed at the H_2/MeOAc molar ratio of 10 in the gasification chamber. The mixture went into the reactor, and the reaction pressure and temperature were controlled at 3.0 MPa and 613 K, respectively. The products were collected and analyzed through a gas chromatograph device (North Branch of Ruili SP-3200A) using a flame ionization detector (FID), equipped with a HJ-WAX capillary column.

2.3. Catalyst characterization

2.3.1. N_2 physisorption

The N_2 physisorption was carried out on Micromeritics Nova 2200e device to analyze the textual properties of the catalysts. First, the samples were heated to 573 K and outgassed for 4 h at the condition of vacuum. Then the N_2 adsorption–desorption isotherms for the catalysts were measured at the temperature of 77 K. The specific surface area was calculated according to the isotherms using the BET method, and the pore volume and pore size were calculated by BJH method on the basis of the desorption branches of the nitrogen isotherms.

2.3.2. N_2O chemisorption

The copper surface area and dispersion of calcined samples were measured by a pulse titration method using the adsorption and decomposition of N_2O on a Micromeritics AutoChem 2910 [18–20].

2.3.3. X-ray diffraction

The powdered X-ray diffraction (XRD) profiles were collected on a D/MAX-2500 X-ray diffractometer operated at 40 kV and 40 mA, with $\text{CuK}\alpha$ as the radiation source. The scanned range was from 10° to 90° , with a scanning step of 5° min^{-1} . The Cu species crystallite size was calculated by the Scherrer equation.

2.3.4. H_2 -temperature programmed reduction

H_2 -temperature programmed reduction (H_2 -TPR) patterns were obtained on the Micromeritics AutoChem 2910 chemisorption apparatus. Prior to the measurement, the catalysts were pretreated at the temperature of 373 K for 1 h using argon gas. Then the catalysts were reduced by 5 vol.% H_2/Ar from 373 K up to 1173 K, by a heating rate of 10 K min^{-1} .

2.3.5. CO_2 -temperature programmed desorption

CO_2 -temperature programmed desorption (CO_2 -TPD) technique was used to analyze the basicity of catalysts on a Micromeritics AutoChem 2910 instrument. The main steps were as follows. (1) Hundred milligram catalyst sample was reduced for 4 h by 5 vol.% H_2/Ar at 723 K and then cooled to 373 K. (2) The gas was switched to CO_2 for 1 h. (3) Using pure Ar swept to remove weakly adsorbed CO_2 at room temperature. (4) CO_2 -TPD was performed from 300 K to 1173 K by 10 K min^{-1} under an atmosphere of Ar.

2.3.6. X-ray photoelectron spectroscopy

X-ray photoelectron spectroscopy (XPS) and Auger electron spectroscopy (XAES) were recorded on the PHI5000 Versa Probe spectrometer equipped with a electron energy analyzer and a monochromated $\text{Al K}\alpha$ X-ray radiation source ($h\nu = 1486.6\text{ eV}$). All binding energies were referenced to contaminant carbon ($\text{C}1s = 284.8\text{ eV}$). To investigating the catalysts surface states of Cu species at the reaction conditions, XPS spectra were collected for the reduced catalysts. There were $\pm 0.2\text{ eV}$ errors in the process of experiment.

3. Results and discussion

3.1. Catalytic performance of the catalysts

The effects of magnesium oxide amounts on the catalytic activities of $\text{Cu}/x\text{MgO-SiO}_2$ catalysts for hydrogenation of methyl acetate are shown in Fig. 1a and b. The results show that the catalytic activities obtained by $\text{Cu}/x\text{MgO-SiO}_2$ catalysts are better than that of the Cu/SiO_2 catalyst, which indicate that using the composite supports to replace the single support is favorable for ethanol production. When the MgO/SiO_2 mass ratio is 9, the conversion of methyl acetate reaches 80.3% and the selectivity of ethanol is above 99%, which are considerably better than the results of the Cu/SiO_2 and Cu/MgO catalysts under the same reaction conditions. It can be seen from Fig. 1a, there are obvious decline in the catalytic performance curves for $\text{Cu}/1\text{MgO-SiO}_2$, $\text{Cu}/20\text{MgO-SiO}_2$ and Cu/MgO catalysts and obvious decline in the initial two hours for $\text{Cu}/3\text{MgO-SiO}_2$ and $\text{Cu}/9\text{MgO-SiO}_2$ catalysts. The two reasons may account for this phenomenon, the content of Cu on the catalyst surface decreased after undergoing reactions and carbon deposition.

In order to further illustrate the promoted behavior of modified Cu/SiO_2 catalyst, a long-term stability for $\text{Cu}/9\text{MgO-SiO}_2$ catalysts are carried out and displayed in Fig. 1c. It is evident that during 50 h longterm test, methyl acetate conversion shows a slight decrease

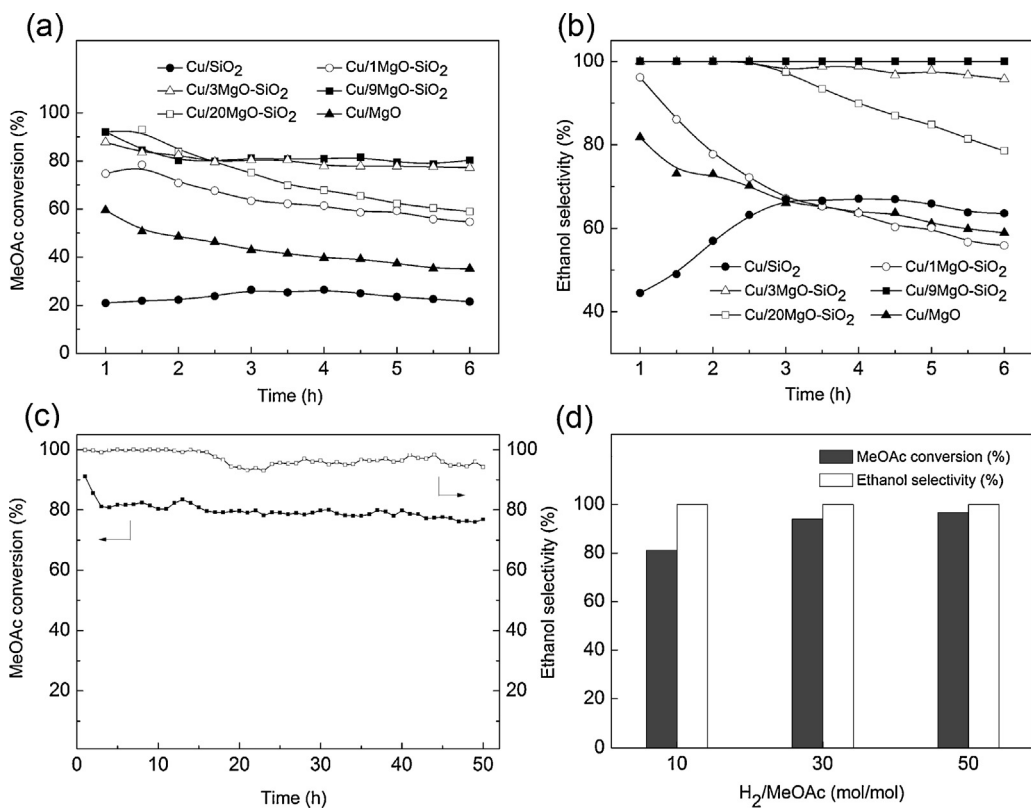
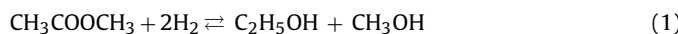


Fig. 1. (a–c) Catalytic performance of Cu/xMgO-SiO₂ catalysts. Reaction conditions: $P=3$ MPa, $T=613$ K, $H_2/MeOAc=10$ (mol/mol), LHSV = 2.0 h⁻¹; (d) Effect of the $H_2/MeOAc$ on the catalytic performance of the Cu/9MgO-SiO₂ catalyst. Reaction conditions: $P=3$ MPa, $T=613$ K, GHSV = 1800 h⁻¹.

from 80 to 76%; In the meantime, ethanol selectivity remains at about 97%. The results indicate that Cu/9MgO-SiO₂ catalyst performs a better catalytic performance.

The influence of $H_2/MeOAc$ molar ratio on the performance of the Cu/9MgO-SiO₂ catalyst was also studied. The results are showed in Fig. 1d. As shown in Fig. 1d, the conversion of MeOAc increases with increasing molar ratio of $H_2/MeOAc$, while the selectivity to ethanol remains unchanged. When the $H_2/MeOAc$ molar ratio is 50, the MeOAc conversion reaches 96.7%, with the ethanol selectivity of 99.0%. The Reaction (1) describes the hydrogenation of methyl acetate to ethanol process.



It can be found that the chemical equilibrium shifts to positive direction with the increase of the H_2 molar contents, so the Cu/9MgO-SiO₂ catalyst can exhibit a much better catalytic activity with increasing $H_2/MeOAc$ molar ratio at constant LHSV (liquid hour space velocity).

3.2. Catalyst characterization

3.2.1. Textural properties of catalysts

The textural properties of different composite MgO-SiO₂ supported Cu-based catalysts are summarized in Table 1. The Cu/SiO₂ sample possess relatively large pore volume of 0.79 cm³ g⁻¹ and relatively high BET surface area of 356.6 m² g⁻¹, whereas those for Cu/MgO are only 30.0 m² g⁻¹ and 0.16 cm³ g⁻¹. The pore volume and BET surface area of Cu/xMgO-SiO₂ are between Cu/SiO₂ and Cu/MgO, and gradually decrease with the increased content of magnesium oxide. The Cu/9MgO-SiO₂ catalyst exhibits the best catalytic activity, however, the pore volume and surface area of this catalyst are ordinary. It can be concluded from the above facts that textural properties, such as surface area and pore volume, are not

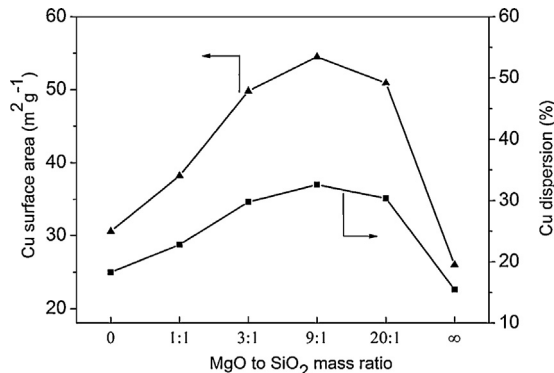


Fig. 2. Copper surface area and dispersion versus support composition.

the primary factors that determine the catalytic performance. The key factors which mainly influence the catalytic performance may be more chemical properties than physical properties.

The copper dispersion and surface area of Cu/SiO₂ and Cu/xMgO-SiO₂ catalysts measured by N₂O adsorption are shown in Table 1 and Fig. 2. The copper dispersion and surface area increase with the increased magnesium oxide content and maximize when the MgO/SiO₂ mass ratio is 9, and then decline with further increasing in magnesium oxide content. The various copper dispersion and surface area may be caused by different content of magnesium oxide which is used as a kind of isolating agent to suppress aggregation of copper species during the activation of catalysts and hydrogenation of MeOAc. The Cu/9MgO-SiO₂ catalyst demonstrates a best catalytic activity that may be due to the acquired maximum copper dispersion and surface. In dimethyl oxalate hydrogenation, Yin et al. [21] reported that 20 wt% Cu catalyst exhibited a best catalytic performance while it possessed a max-

Table 1Physicochemical properties of Cu/xMgO-SiO₂ catalysts.

Catalyst	<i>S</i> _{BET} (m ² g ⁻¹)	<i>V</i> _P (cm ³ g ⁻¹)	<i>d</i> _P (nm)	Cu dispersion ^a (%)	<i>S</i> _{Cu^a} (m ² g ⁻¹ cat)	<i>d</i> _{CuO^b} (nm)	<i>d</i> _{M^b} (nm)
Cu/SiO ₂	356.6	0.79	20.2	18.3	30.6	20.9	20.9
Cu/1MgO-SiO ₂	222.9	0.53	16.1	22.8	38.2	19.0	18.8
Cu/3MgO-SiO ₂	110.7	0.20	14.6	29.8	49.8	14.5	13.2
Cu/9MgO-SiO ₂	64.7	0.22	13.9	32.6	54.5	—	—
Cu/20MgO-SiO ₂	52.7	0.21	16.1	30.4	50.9	—	—
Cu/MgO	30.0	0.16	21.1	15.5	26.0	—	—

^a Cu dispersion and surface area of Cu determined by N₂O titration.^b CuO and Cu crystallite sizes calculated using the Scherrer formula.

imum copper dispersion and surface, and identified that copper dispersion and surface may promote its catalytic performance.

3.2.2. Crystalline phase

The XRD patterns of all the samples after calcination are shown in Fig. 3a. When MgO to SiO₂ mass ratio is lower than 3, the characteristic peaks at 2θ of 35.6° and 38.7° (JCPDS 05-0661) are ascribed to CuO, indicating that some copper species are agglomerated on the surface of the support. With the continuous increasing of magnesium oxide content, new diffraction peaks at 2θ of 36.9°, 42.9°, and 62.2° (JCPDS 43-1022) attributed to magnesium oxide become apparent, whereas CuO diffraction peaks disappear, indicating the copper species are highly dispersed in MgO-SiO₂ support. The CuO particle sizes calculated by Scherrer equation are shown in Table 1. Since the crystalline sizes of copper species are quite small, the diffraction peak can not be detected. The peak intensity and sharpness increase along with the increasing particle sizes. According to this situation, the CuO crystallite sizes of the Cu/xMgO-SiO₂ catalysts are much smaller than the Cu/SiO₂ catalyst, which illustrate that the employ of composite MgO-SiO₂ support can reduce particle size to promote copper particles dispersed.

The XRD patterns of reduced catalysts are presented in Fig. 3b. Some diffraction peaks at 2θ of 43.3°, 50.4°, and 74.1° attributed to Cu⁰ (JCPDS 04-0836) are observed. The intensities of Cu⁰ diffraction peaks weaken or even disappear with an increasing MgO/SiO₂ mass ratio, but the diffraction peaks are very distinct for Cu/MgO sample. The Cu⁰ crystallite size estimated as shown in Table 1 by the Scherrer equation decreases along with the increased magnesium oxide when the MgO/SiO₂ mass ratio is lower than 20. Obviously, the results demonstrate that adding moderate magnesium oxide to catalysts is beneficial for inhibiting growth of metallic copper particles. Moreover, a weak peak at 2θ of 36.6° attributed to Cu₂O (JCPDS 05-0667) is observed when MgO/SiO₂ mass ratio is above 1, and the peak becomes apparent with an increasing MgO/SiO₂ mass ratio, and Cu/MgO catalyst sample exhibits the most obvious Cu₂O characteristic peak. The results indicate that the metallic Cu and Cu₂O coexist in the working catalysts, and the ratio of Cu⁺/(Cu⁺ + Cu⁰) significantly change with increasing magnesium oxide content. It can be concluded that the catalytic activity may be associated with the Cu valence states distribution and other chemical properties.

3.2.3. Reducibility and surface base properties

To evaluate the reduction behavior of the catalysts, the calcined Cu/SiO₂, Cu/MgO and Cu/xMgO-SiO₂ samples were examined by H₂-TPR and the result are presented in Fig. 4a. In Cu/SiO₂ catalyst, the reduction peak centered at 576 K can be identified as CuO → Cu⁰. In many open literatures, this reduction peak is ascribed to the process of reducing small CuO clusters. Wang et al. [22] reported Cu/SiO₂ catalyst prepared by impregnation method presented three different temperature of TPR peaks (518 K, 560 K, and 629 K). The two lower reduced peaks can be tentatively ascribed to small CuO clusters and highly dispersed copper species; The reduced peak at 629 K may be caused by reduction

of larger CuO clusters. For Cu/SiO₂ catalyst, the 576 K reduced peaks may be ascribed to collective action of the reduction of above mentioned Cu species. The Cu/MgO sample exhibits a broad reduction peak at 739 K along with a shoulder peak at 677 K, indicating that the sample is reduced in two stages, i.e., CuO → Cu₂O and Cu₂O → Cu⁰. The broad peak may be ascribed to collective action of reducing Cu⁺ and CuO clusters to Cu⁰. A similar behavior was reported by Nagaraja et al. [23] for Cu/MgO catalyst prepared by co-precipitation method that Cu/MgO sample was reduced in two steps. For Cu/xMgO-SiO₂ samples, the reduction peak is shifted to higher temperature with increasing magnesium oxide amount. However, it lies between Cu/SiO₂ and Cu/MgO. A similar result was also reported by Tu and Chen [17] that the reduction temperature of Cu-MgO/SiO₂ was higher than that of Cu/SiO₂. This result is possibly due to the addition of MgO into Cu/SiO₂ catalyst, which essentially improves the dispersion of cupreous species during the preparation of catalysts, strengthens the interaction between active components of copper ions and catalyst support. The enhanced interaction makes catalysts more difficult to be reduced to Cu⁰, and alters Cu valence states distribution on catalyst surface.

Temperature programmed desorption (TPD) of CO₂ is a common technique to determine the basicity of solid catalysts. The basicity of Cu/SiO₂ and Cu/xMgO-SiO₂ catalysts obtained by CO₂-TPD and the profiles are displayed in Fig. 4b. Cu/SiO₂ sample exhibits two CO₂ desorption peaks, a low-temperature peak of 550–700 K and a high desorption peaks of 750–950 K, which can be identified as moderate and strong basic sites, respectively. For Cu/xMgO-SiO₂ catalysts, added magnesium oxide can lead to the appearance of weak basic sites with a CO₂ desorption peak at 300–500 K and the disappearance of the moderate basic sites with a CO₂ desorption peak at 550–700 K. Strong basic sites with a CO₂ desorption peak at 950–1050 K gradually disappears when the content of magnesium oxide increases. Tu and Chen [17] found that the addition of magnesium oxide to Cu/SiO₂ catalyst could increase the content of weak basic site of catalyst and Cu-MgO/SiO₂ catalyst exhibited better catalytic stability than Cu/SiO₂ in the dehydrogenation reaction process, which was mainly attributed to beneficial effects of weakly basic sites on Cu species, while the strong basic sites could damage the stabilities of the catalysts. It can be found that Cu/9MgO-SiO₂ catalyst exhibits more weak basic sites, so the excellent catalytic activity may be associated with it.

3.2.4. Surface chemical states

XPS and XAES were recorded to analyze the chemical state and surface composition of activated catalysts. The XPS curves of activated Cu/xMgO-SiO₂ are shown in Fig. 5a. Generally, the peak at binding energy of around 934 eV and the 2p → 3d satellite peak at 942–944 eV are the proofs of existing Cu²⁺ [24]. However, the above two peaks can not be found and the peak at 932 eV is observed, which may be due to the reduction of Cu²⁺ to Cu⁺ or Cu⁰ species. In addition, the tiny chemical shift of binding energy for Cu2p_{3/2}

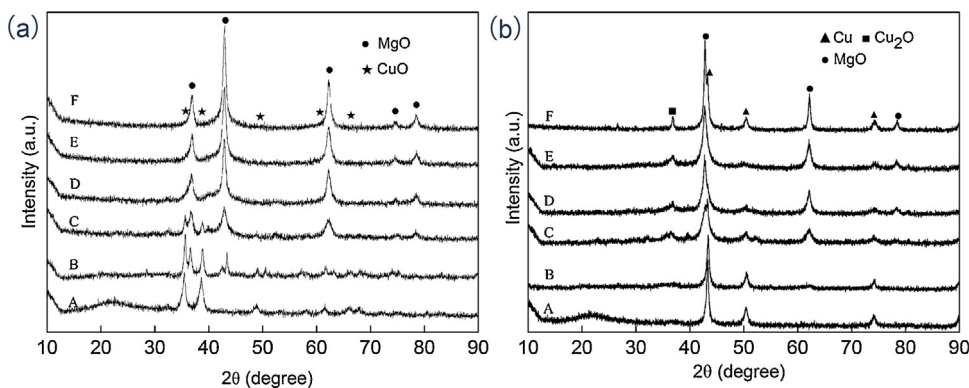


Fig. 3. (a) XRD patterns of the calcined Cu/xMgO-SiO₂ catalysts; (b) XRD patterns of the reduced Cu/xMgO-SiO₂ catalysts.
(A) Cu/SiO₂; (B) Cu/1MgO-SiO₂; (C) Cu/3MgO-SiO₂; (D) Cu/9MgO-SiO₂; (E) Cu/20MgO-SiO₂; (F) Cu/MgO.

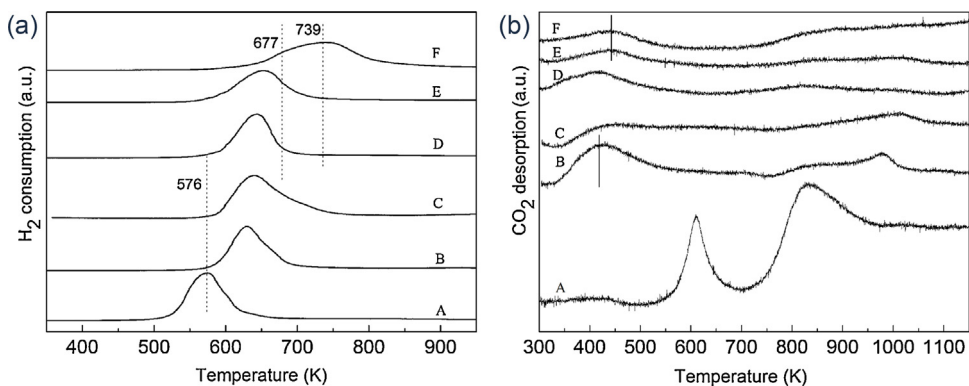


Fig. 4. (a) H₂-TPR profiles of the calcined Cu/xMgO-SiO₂ catalysts. (b) CO₂-TPD patterns of Cu/xMgO-SiO₂ catalysts.
(A) Cu/SiO₂; (B) Cu/1MgO-SiO₂; (C) Cu/3MgO-SiO₂; (D) Cu/9MgO-SiO₂; (E) Cu/20MgO-SiO₂; (F) Cu/MgO.

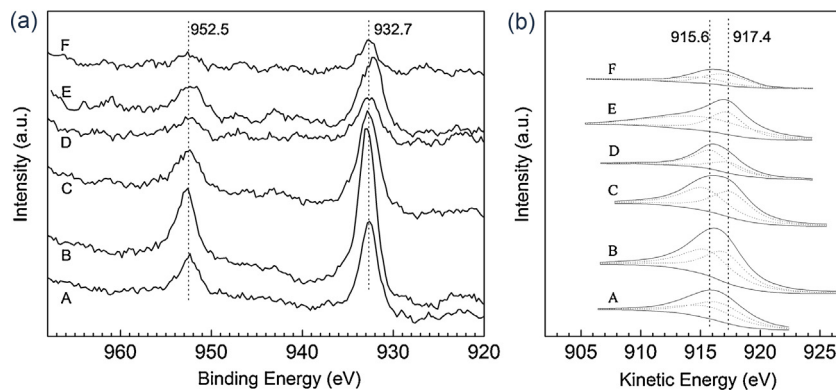


Fig. 5. (a) Cu2p XPS spectra of the reduced Cu/xMgO-SiO₂ catalysts; (b) Cu LMM XAES spectra of the reduced Cu/xMgO-SiO₂ catalysts.
(A) Cu/SiO₂; (B) Cu/1MgO-SiO₂; (C) Cu/3MgO-SiO₂; (D) Cu/9MgO-SiO₂; (E) Cu/20MgO-SiO₂; (F) Cu/MgO.

occurs, which may be caused by the interaction of Cu species and support.

The binding energy distinction is very minimal between Cu⁰ and Cu⁺. Thus, the kinetic energy of the Cu LMM and the binding energy of the Cu2p_{3/2} together make up an Auger parameter α_1 , which is used to distinguish Cu⁺ and Cu⁰ that existing on the catalyst surface. In general, α_1 is ca. 1849.0 eV for Cu⁰ and ca. 1847.0 eV for Cu⁺ [21,25,26]. In the Cu LMM XAES spectra of activated catalysts (Fig. 5b), Auger kinetic energy peaks ranging from 905 to 925 eV are observed, strongly indicating the Cu⁰ and Cu⁺ are coexisting on the catalysts surface. The results of the Cu⁺ molar content estimated from the deconvolution are shown in Table 2. The addition

Table 2
Surface Cu component of the reduced catalysts based on Cu LMM XAES spectra.

Catalyst	KE ^a (eV)		AP ^b (eV)		Cu2p _{3/2}	X _{Cu⁺} ^c (%)
	Cu ⁺	Cu ⁰	Cu ⁺	Cu ⁰		
Cu/SiO ₂	915.8	916.6	1848.4	1849.2	932.6	44.4
Cu/1MgO-SiO ₂	915.6	917.0	1848.5	1849.9	932.9	50.4
Cu/3MgO-SiO ₂	915.2	917.6	1848.1	1850.5	932.9	52.6
Cu/9MgO-SiO ₂	915.6	917.4	1848.5	1850.3	932.9	63.9
Cu/20MgO-SiO ₂	915.3	917.2	1847.7	1849.6	932.4	56.1
Cu/MgO	915.0	917.0	1847.9	1849.9	932.9	45.9

^a Kinetic energy.

^b Auger parameter.

^c $X_{Cu^+} = Cu^+/(Cu^0 + Cu^+) \times 100\%$.

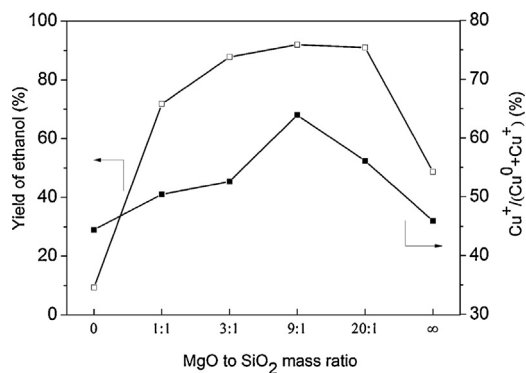


Fig. 6. Yield of ethanol and $\text{Cu}^+/\text{Cu}^0+\text{Cu}^+$ versus support composition.

of magnesium oxide results in a change of the $\text{Cu}^+/\text{Cu}^0+\text{Cu}^+$ molar content on the catalyst surface, following the order: Cu/9MgO-SiO₂ (63.9%) > Cu/20MgO-SiO₂ (56.1%) > Cu/3MgO-SiO₂ (52.6%) > Cu/MgO-SiO₂ (50.4%) > Cu/MgO (45.9%) > Cu/SiO₂ (44.4%). The Cu/9MgO-SiO₂ catalyst exhibits the maximum the molar content of $\text{Cu}^+/\text{Cu}^0+\text{Cu}^+$. The large amount of Cu⁺ species existing in the reduction catalysts signifies that the interaction between copper species and support is strong, which hinders the reduction of Cu²⁺ or Cu⁺ to Cu⁰. It is clearly indicated that the added magnesium oxide amount generate huge effects on the distributions of Cu⁺ and Cu⁰ on the catalyst surface. TPR and XPS results are agreed on the issues.

Fig. 6 also presents the yield of ethanol and $\text{Cu}^+/\text{Cu}^0+\text{Cu}^+$ as a function of the MgO to SiO₂ mass ratio. It shows that the change of catalytic performance and molar ratio of $\text{Cu}^+/\text{Cu}^0+\text{Cu}^+$ with increasing magnesium oxide amount are all volcanic form. When MgO to SiO₂ mass ratio is 9, the highest $\text{Cu}^+/\text{Cu}^0+\text{Cu}^+$ ratio can be obtained, while this catalyst possesses a best catalytic activity (the ethanol yield of 92%), which implies that a large amount of Cu⁺ species play an important role in the process of the catalytic hydrogenation of methyl acetate to ethanol. In methyl acetate hydrogenation, Poels and Brands [27] reported that Cu⁰ sites adsorbed hydrogen molecules, and Cu⁺ sites strongly bound and activated the methoxy and the acyl groups. In dimethyl oxalate hydrogenation, Chen et al. [28] identified that a cooperative effect existed between Cu⁺ and Cu⁰ and it was the main reason for improving their activities in the hydrogenation of DMO. Thus, the catalytic activity is linked to the content of Cu⁰ and Cu⁺. For methyl acetate hydrogenation to ethanol, catalytic performance is a result of synergistic effect between Cu⁰ and Cu⁺. It is inferred that the process of Cu⁺ sites activated methoxy and acyl groups is the control step of the reaction. So the large amount of Cu⁺ species is proposed to be the main reason for the improved catalytic performance.

4. Conclusions

A series of Cu/MgO-SiO₂ catalysts with different support compositions of MgO and SiO₂ were prepared by the ammonia-evaporation method and evaluated for methyl acetate hydrogenation to ethanol. Among all catalysts tested, Cu/9MgO-SiO₂ catalyst

displayed the best catalytic performance. The characterization analysis show that, adding magnesium oxide to Cu/SiO₂ catalyst can improve Cu surface area and dispersion, on the other hand, can increase content of surface Cu⁺ sites through strengthening the interaction between copper species and support. The maximum molar ratio of $\text{Cu}^+/\text{Cu}^0+\text{Cu}^+$ obtained by tuning the magnesium oxide content can lead to the highest catalytic performance. Therefore, the large Cu surface area, Cu dispersion, amount of weakly basic sites and Cu⁺ species are believed to the main reasons for improving catalytic performance in the hydrogenation of methyl acetate to ethanol.

Acknowledgements

We gratefully acknowledge the financial supports from Major State Basic Research Program of China (2012CB720300), and Program for Changjiang Scholars and Innovative Research Team in University (IRT1161).

References

- [1] J. Goldemberg, Science 315 (2007) 808–810.
- [2] J. Gong, H. Yue, Y. Zhao, S. Zhao, L. Zhao, J. Lv, S. Wang, X. Ma, J. Am. Chem. Soc. 134 (2012) 13922–13925.
- [3] S. Zhao, H. Yue, Y. Zhao, B. Wang, Y. Geng, J. Lv, S. Wang, J. Gong, X. Ma, J. Catal. 297 (2013) 142–150.
- [4] H. Yue, X. Ma, J. Gong, Acc. Chem. Res. 47 (2014) 1483–1492.
- [5] Y.-M. Zhu, L. Shi, J. Ind. Eng. Chem. 20 (2014) 2341–2347.
- [6] Y.-M. Zhu, X.W.L. Shi, Bull. Korean Chem. Soc. 35 (2014) 141–146.
- [7] D. Wang, G. Yang, Q. Ma, Y. Yoneyama, Y. Tan, Y. Han, N. Tsubaki, Fuel 109 (2013) 54–60.
- [8] H. Yue, Y. Zhao, L. Zhao, J. Lv, S. Wang, J. Gong, X. Ma, AIChE J. 58 (2012) 2798–2809.
- [9] X. Ma, H. Chi, H. Yue, Y. Zhao, Y. Xu, J. Lv, S. Wang, J. Gong, AIChE J. 59 (2013) 2530–2539.
- [10] X. Zheng, H. Lin, J. Zheng, X. Duan, Y. Yuan, ACS Catal. 3 (2013) 2738–2749.
- [11] A. Yin, X. Guo, W.-L. Dai, Appl. Catal. A Gen. 377 (2010) 128–133.
- [12] B. Hu, Y. Yamaguchi, K. Fujimoto, Catal. Commun. 10 (2009) 1620–1624.
- [13] R. Yang, Y. Zhang, Y. Iwama, N. Tsubaki, Appl. Catal. A Gen. 288 (2005) 126–133.
- [14] B. Nagaraja, A. Padmasri, B. David Raju, K. Rama Rao, J. Mol. Catal. A Chem. 265 (2007) 90–97.
- [15] B. Nagaraja, V. Siva Kumar, V. Shasikala, A. Padmasri, B. Sreedhar, B. David Raju, K. Rama Rao, Catal. Commun. 4 (2003) 287–293.
- [16] M. Balraj, K. Jagadeeswaran, P.S. Prasad, N. Lingaiah, Catal. Sci. Technol. 2 (2012) 1967–1976.
- [17] Y.-J. Tu, Y.-W. Chen, Ind. Eng. Chem. Res. 37 (1998) 2618–2622.
- [18] S. Xia, Z. Yuan, L. Wang, P. Chen, Z. Hou, Appl. Catal. A Gen. 403 (2011) 173–182.
- [19] G. Chinchen, C. Hay, H. Vandervell, K. Waugh, J. Catal. 103 (1987) 79–86.
- [20] C. Van Der Grift, A. Wielaars, B. Jogh, J. Van Beunum, M. De Boer, M. Versluijs-Helder, J. Geus, J. Catal. 131 (1991) 178–189.
- [21] A. Yin, X. Guo, W.-L. Dai, K. Fan, J. Phys. Chem. C 113 (2009) 11003–11013.
- [22] Z. Wang, Q. Liu, J. Yu, T. Wu, G. Wang, Appl. Catal. A Gen. 239 (2003) 87–94.
- [23] B. Nagaraja, V. Siva Kumar, V. Shasikala, A. Padmasri, S. Sreevardhan Reddy, B. David Raju, K. Rama Rao, J. Mol. Catal. A Chem. 223 (2004) 339–345.
- [24] A. Gervasini, M. Manzoli, G. Martra, A. Ponti, N. Ravasio, L. Sordelli, F. Zuccheri, J. Phys. Chem. B 110 (2006) 7851–7861.
- [25] A. Yin, X. Guo, W.-L. Dai, K. Fan, J. Phys. Chem. C 114 (2010) 8523–8532.
- [26] Z. He, H. Lin, P. He, Y. Yuan, J. Catal. 277 (2011) 54–63.
- [27] E. Poels, D. Brands, Appl. Catal. A Gen. 191 (2000) 83–96.
- [28] L.-F. Chen, P.-J. Guo, M.-H. Qiao, S.-R. Yan, H.-X. Li, W. Shen, H.-L. Xu, K.-N. Fan, J. Catal. 257 (2008) 172–180.